



A Neuroligin-3 Mutation Implicated in Autism Increases Inhibitory Synaptic Transmission in Mice

Katsuhiko Tabuchi, *et al.*
Science **318**, 71 (2007);
DOI: 10.1126/science.1146221

The following resources related to this article are available online at www.sciencemag.org (this information is current as of March 27, 2008):

Updated information and services, including high-resolution figures, can be found in the online version of this article at:

<http://www.sciencemag.org/cgi/content/full/318/5847/71>

Supporting Online Material can be found at:

<http://www.sciencemag.org/cgi/content/full/1146221/DC1>

A list of selected additional articles on the Science Web sites **related to this article** can be found at:

<http://www.sciencemag.org/cgi/content/full/318/5847/71#related-content>

This article **cites 35 articles**, 14 of which can be accessed for free:

<http://www.sciencemag.org/cgi/content/full/318/5847/71#otherarticles>

This article has been **cited by** 2 article(s) on the ISI Web of Science.

This article has been **cited by** 5 articles hosted by HighWire Press; see:

<http://www.sciencemag.org/cgi/content/full/318/5847/71#otherarticles>

This article appears in the following **subject collections**:

Medicine, Diseases

<http://www.sciencemag.org/cgi/collection/medicine>

Information about obtaining **reprints** of this article or about obtaining **permission to reproduce this article** in whole or in part can be found at:

<http://www.sciencemag.org/about/permissions.dtl>

A Neuroligin-3 Mutation Implicated in Autism Increases Inhibitory Synaptic Transmission in Mice

Katsuhiko Tabuchi,¹ Jacqueline Blundell,² Mark R. Etherton,¹ Robert E. Hammer,³ Xinran Liu,¹ Craig M. Powell,^{2,4} Thomas C. Südhof^{1,5,6*}

Autism spectrum disorders (ASDs) are characterized by impairments in social behaviors that are sometimes coupled to specialized cognitive abilities. A small percentage of ASD patients carry mutations in genes encoding neuroligins, which are postsynaptic cell-adhesion molecules. We introduced one of these mutations into mice: the Arg⁴⁵¹→Cys⁴⁵¹ (R451C) substitution in neuroligin-3. R451C mutant mice showed impaired social interactions but enhanced spatial learning abilities. Unexpectedly, these behavioral changes were accompanied by an increase in inhibitory synaptic transmission with no apparent effect on excitatory synapses. Deletion of neuroligin-3, in contrast, did not cause such changes, indicating that the R451C substitution represents a gain-of-function mutation. These data suggest that increased inhibitory synaptic transmission may contribute to human ASDs and that the R451C knockin mice may be a useful model for studying autism-related behaviors.

Autism is a widespread cognitive disorder characterized by impairments in social interactions, including verbal communication and social play, and can be accompanied by stereotyped patterns of behavior (1–3). Autism is a heterogeneous condition, prompting the designation of ASDs. Individuals with ASDs occasionally show enhanced cognitive abilities [autistic savant syndrome (4)]. At the other end

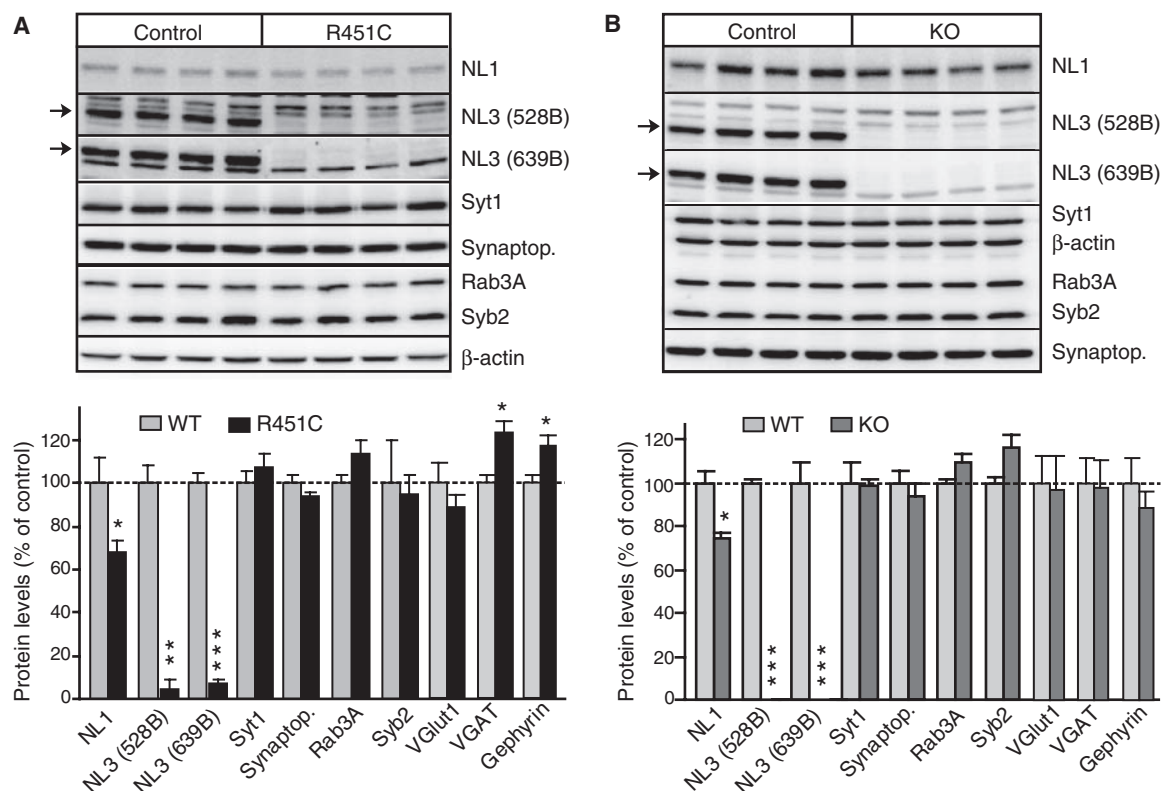
of the spectrum, ASDs are often associated with mental retardation, and the symptoms of ASDs are part of several neurological diseases, such as fragile X and Rett syndromes (5–7). Genetics strongly contributes to ASDs (1, 2), and a small number of cases with idiopathic ASD are associated with mutations in a single gene, including genes encoding neuroligins and their associated proteins (8).

Neuroligins are a family of postsynaptic cell-adhesion molecules that are ligands (or receptors, depending on the perspective) for neurexins, another class of synaptic cell-adhesion molecules (9, 10). Humans express five neuroligins, including neuroligin-3, an X-chromosomal gene that undergoes regular X inactivation, and neuroligin-4 and -5, which are encoded by a pair of pseudoautosomal genes on the X and Y chromosomes (11). Mice express close homologs to human neuroligin-1, -2, and -3 (9) and a fourth isoform that appears to be more distantly related to other neuroligins (GenBank accession number EF692521) (11). Neuroligin-1 and -2 are differentially localized to excitatory or inhibitory synapses (12–14). Overexpression of neuroligins in transfected neurons increases synapse numbers and the frequency of spontaneous synaptic events (15–20). Consistent with their localizations, overexpression of neuroligin-1 enhances only excitatory synaptic transmission, whereas overexpression of neuroligin-2 enhances only inhibitory synaptic transmission

¹Department of Neuroscience, University of Texas Southwestern Medical Center, Dallas, TX 75390, USA. ²Department of Neurology, University of Texas Southwestern Medical Center, Dallas, TX 75390, USA. ³Department of Biochemistry, University of Texas Southwestern Medical Center, Dallas, TX 75390, USA. ⁴Department of Psychiatry, University of Texas Southwestern Medical Center, Dallas, TX 75390, USA. ⁵Department of Molecular Genetics, University of Texas Southwestern Medical Center, Dallas, TX 75390, USA. ⁶Howard Hughes Medical Institute, University of Texas Southwestern Medical Center, Dallas, TX 75390, USA.

*To whom correspondence should be addressed. E-mail: thomas.sudhof@utsouthwestern.edu

Fig. 1. Generation and characterization of neuroligin-3 R451C KI and neuroligin-3 KO mice. (A and B) Representative immunoblots and summary graphs of protein levels in the brains of neuroligin-3 R451C KI mice (A) and neuroligin-3 KO mice (B). Selected synaptic proteins (NL1, neuroligin-1; NL3, neuroligin-3; Synaptop., synaptophysin; Syt1, synaptotagmin-1; and Syb2, synaptobrevin-2) were analyzed by quantitative immunoblotting; two different neuroligin-3 antibodies were used (528B and 639B; arrows point to neuroligin-3 band; data shown are means \pm SEMs; $n = 4$ littermate pairs; * $P < 0.05$; ** $P < 0.01$; *** $P < 0.005$ by Student's t test).



(20). Deletion of neuroligin-1 or -2 in mice causes corresponding selective decreases in excitatory or inhibitory synaptic transmission, respectively, but no significant synapse loss, whereas neuroligin-3 has not been examined (11, 21).

Missense and nonsense mutations in neuroligin-3 and -4 have been identified in a subset of human patients with ASDs (22–24). One of these mutations, the Arg⁴⁵¹→Cys⁴⁵¹ (R451C) substitution in neuroligin-3, alters a conserved residue in the extracellular esterase-homology domain of neuroligin-3 (22). In transfected neurons, the R451C substitution causes partial retention of neuroligin-3 in the endoplasmic reticulum but does not abolish its ability to promote synapse formation (20, 25, 26). In addition, an internal deletion in the gene encoding neuexin-1 that interacts with neuroligins was connected to ASDs (27), and three different nonsense mutations in Shank3, an intracellular binding partner for neuroligins, were also found in patients with

ASDs (28). Thus, in rare instances mutations in three gene families that encode neuroligins or their interacting proteins are associated with familial idiopathic ASDs.

An increase in inhibitory synapse markers in R451C mutant mice. Autism is thought to arise from functional changes in neural circuitry and to be associated with an imbalance between excitatory and inhibitory synaptic transmission, but the mechanisms involved are unknown (29). To investigate possible mechanisms, we introduced the R451C substitution into the endogenous neuroligin-3 gene in mice by gene targeting, generating R451C knockin (KI) mice (fig. S1) (30). Moreover, to test whether the R451C substitution represents a gain- or a loss-of-function change, we also analyzed neuroligin-3 knockout (KO) mice (fig. S1). Because the neuroligin-3 gene is X-chromosomal, we performed analyses on male offspring derived from matings of a heterozygous female with a wild-type (WT) male

mouse. Neuroligin-3 R451C KI and neuroligin-3 KO mice were viable and fertile and exhibited no obvious abnormalities or premature mortality (fig. S2) (11).

We first analyzed the amounts of neuroligin-3 and of other synaptic proteins in neuroligin-3 R451C KI and KO mice. The R451C substitution caused a decrease in neuroligin-3 of ~90% in forebrain as measured by quantitative immunoblotting with two different antibodies, whereas the KO caused a complete loss of neuroligin-3 (Fig. 1). In addition, we observed a small decrease in neuroligin-1 in both the KI and the KO mice and a significant increase in the levels of two markers for inhibitory synapses [the vesicular γ -aminobutyric acid (GABA) transporter VGAT and the postsynaptic protein gephyrin] in the KI mice, whereas no increases in VGAT or gephyrin levels were detected in the KO mice (Fig. 1). No significant change in the levels of other proteins examined were observed, in par-

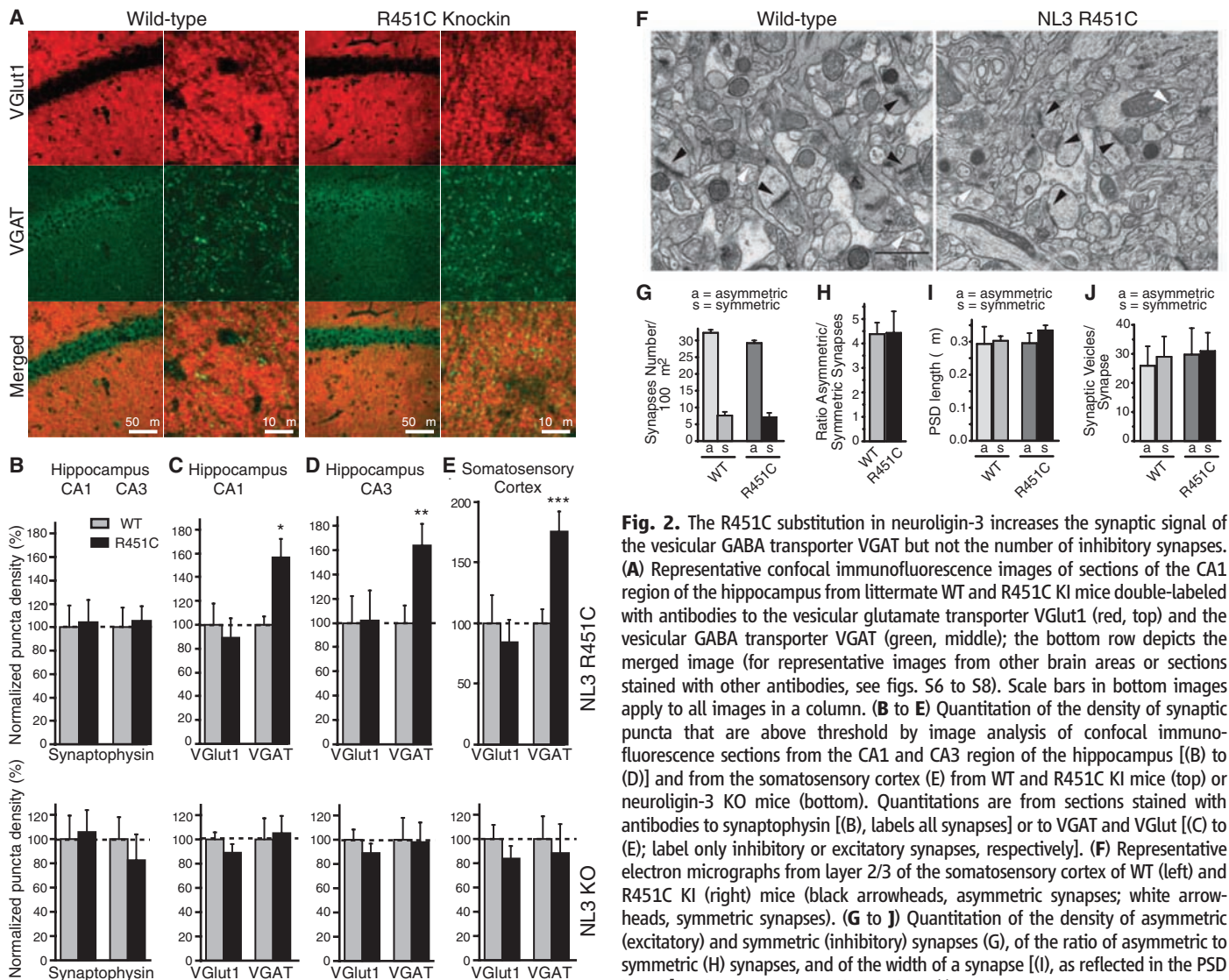


Fig. 2. The R451C substitution in neuroligin-3 increases the synaptic signal of the vesicular GABA transporter VGAT but not the number of inhibitory synapses. (A) Representative confocal immunofluorescence images of sections of the CA1 region of the hippocampus from littermate WT and R451C KI mice double-labeled with antibodies to the vesicular glutamate transporter VGlut1 (red, top) and the vesicular GABA transporter VGAT (green, middle); the bottom row depicts the merged image (for representative images from other brain areas or sections stained with other antibodies, see figs. S6 to S8). Scale bars in bottom images apply to all images in a column. (B to E) Quantitation of the density of synaptic puncta that are above threshold by image analysis of confocal immunofluorescence sections from the CA1 and CA3 region of the hippocampus [(B) to (D)] and from the somatosensory cortex (E) from WT and R451C KI mice (top) or neuroligin-3 KO mice (bottom). Quantitations are from sections stained with antibodies to synaptophysin [(B), labels all synapses] or to VGAT and VGlut1 [(C) to (E); label only inhibitory or excitatory synapses, respectively]. (F) Representative electron micrographs from layer 2/3 of the somatosensory cortex of WT (left) and R451C KI (right) mice (black arrowheads, asymmetric synapses; white arrowheads, symmetric synapses). (G to J) Quantitation of the density of asymmetric (excitatory) and symmetric (inhibitory) synapses (G), of the ratio of asymmetric to symmetric (H) synapses, and of the width of a synapse [(I), as reflected in the PSD length] and its synaptic vesicle numbers (J) in electron micrographs from three

pairs of littermate WT and R451C KI mice [data shown in (B) to (E) and (G) to (J) are means \pm SEMs; $n = 3$ littermate pairs; * $P < 0.05$; ** $P < 0.01$; *** $P < 0.005$ by Student's t test]. PSD, postsynaptic density.

ticular no change in the levels of the vesicular glutamate transporter or other proteins characteristic of excitatory synapses (Fig. 1 and figs. S3 and S4) (30). These data suggest that the neuroligin-3 R451C KI and KO did not cause a global change in the molecular composition of the brain, except for a small increase in inhibitory markers in the KI but not the KO mice.

The decreased concentrations of R451C mutant neuroligin-3 could be due to a destabilization of the mutant protein. Alternatively, because the construction of the R451C KI mice involved the introduction of loxP and flr recombination sites

into the neuroligin-3 gene intron, it is possible that the genetic manipulation may have impaired expression of neuroligin-3. To differentiate between these two possibilities, we measured the messenger RNA (mRNA) levels of neuroligin-3 in WT and R451C KI mice by using quantitative reverse transcription polymerase chain reaction (RT-PCR) but detected no decrease of the neuroligin-3 mRNA in the mutant mice (fig. S5). These data indicate that the R451C substitution destabilizes neuroligin-3, consistent with the retention of R451C mutant neuroligin-3 in the endoplasmic reticulum observed in transfection studies (20, 25).

We next examined the R451C mutant brains morphologically but failed to detect a major change in brain architecture (fig. S6). We then measured the intensity of synapse staining by using antibodies to synaptic vesicle proteins. We stained cryostat sections from the somatosensory cortex and from the CA1 and CA3 regions of the hippocampus with antibodies to synaptophysin, a general marker of all synapses, and to the vesicular glutamate transporter VGlut1 and the vesicular GABA transporter VGAT, markers of excitatory and inhibitory synapses, respectively. The staining patterns observed were characteristic for the excitatory and inhibitory synapses in these brain regions, but the intensity for VGAT staining appeared to be brighter in R451C KI mice than in control or in KO mice (Fig. 2A and figs. S7 and S8). To test this, we used an image analysis that estimates the number and size of puncta labeled with the various antibodies above a defined threshold value applied to all images (Fig. 2, B to E, and figs. S7 and S8). We observed a dramatic increase in the number of VGAT-positive puncta in the R451C KI mice in all three brain regions analyzed (50 to 80% increase). In contrast, the number of VGlut1- or synaptophysin-positive puncta above threshold was unchanged, and the average size of the puncta was also not altered for any of the three antibodies (Fig. 2, B to E, and figs. S7 and S8) (30). Moreover, no increase in the density of VGAT-positive puncta was detected in the neuroligin-3 KO mice (Fig. 2, B to E).

The increased number of VGAT-positive puncta above threshold in the R451C KI mice could be due to an increase in inhibitory synapse numbers or a shift in the distribution of VGAT, such that more synapses contain a high concentration of the transporter. To differentiate between these two possibilities, we examined the number and structure of synapses in layer 2/3 of the somatosensory cortex by electron microscopy but detected no major change in synapse number or structure (Fig. 2, F to J). Thus, the R451C substitution does not increase synapse formation but appears to act at a step downstream of synapse formation to increase the average VGAT signal per synapse. This conclusion is also consistent with the fact that neuroligin deletions in general have not been found to alter synapse numbers but instead selectively impair synaptic strength (11, 21).

Inhibitory synaptic strength is increased in neuroligin-3 R451C KI but not KO mice.

We measured synaptic function in the R451C KI mice with whole-cell recordings in layer 2/3 of the somatosensory (barrel) cortex in acute slices. Examination of spontaneous synaptic “mini” events (Fig. 3, A to D) uncovered no significant change in the frequency or size of excitatory events but detected a ~50% increase in the frequency of spontaneous inhibitory events. No change in the amplitude of spontaneous inhibitory events was detected. To determine whether the increased frequency of spontaneous

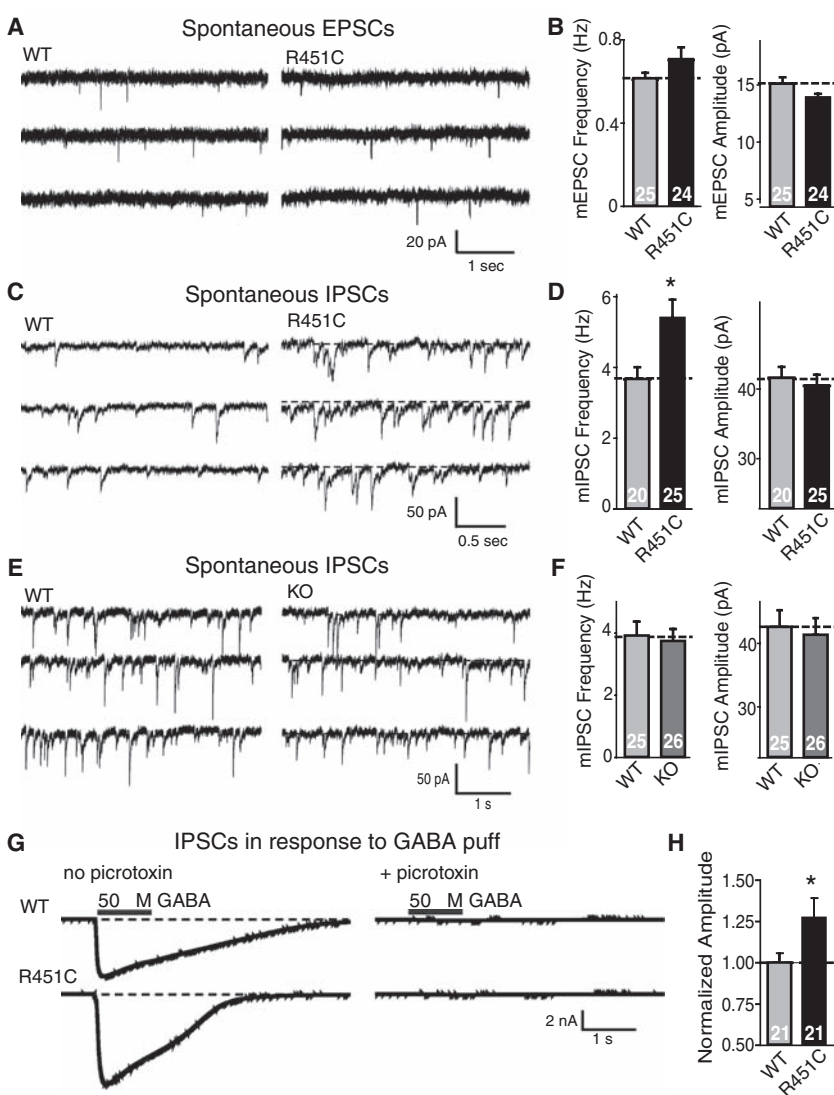


Fig. 3. Neuroligin-3 R451C KI but not neuroligin-3 KO mice exhibit increased spontaneous inhibitory synaptic transmission. Recordings were performed in whole-cell patch-clamp mode in pyramidal neurons in layer 2/3 of the somatosensory cortex in acute slices. Representative traces (A, C, and E) and summary graphs of the amplitudes and frequency (B, D, and F) of spontaneous miniature excitatory postsynaptic currents [mEPSCs; (A) and (B)] and inhibitory postsynaptic currents [mIPSCs; (C) and (D)] from R451C KI [(A) to (D)] or KO mice [(E) and (F)]. (G and H) Representative traces (G) and summary graph for response to a locally applied GABA puff (50 μM injected at 5 psi for 1 s) in layer 2/3 of the somatosensory cortex. In (G), responses are also shown in the presence of 50 μM picrotoxin to document their inhibitory nature (data shown are means ± SEMs; $n = 3$ littermate pairs; total number of cells recorded are indicated within bars; * $P < 0.05$; ** $P < 0.01$; *** $P < 0.005$ by Student's t test; all electrophysiological parameters are listed in table S1).

inhibitory synaptic events is due to the loss of neuroligin-3 induced by the R451C substitution (Fig. 1) or reflects a specific action of the mutant protein, we measured the frequency and size of spontaneous inhibitory mini events in neuroligin-3 KO mice (Fig. 3E). Neuroligin-3 KO mice exhibited no increase in the frequency of spontaneous inhibitory mini events (Fig. 3F).

The selective increase of spontaneous inhibitory events in R451C KI mice agrees with the increase in the levels of inhibitory synaptic proteins (Fig. 1) and the number of inhibitory synapses with VGAT signals above threshold (Fig. 2), suggesting that inhibitory synaptic transmission may be enhanced by the R451C substitution. Consistent with this hypothesis, the amplitude of the response to exogenous GABA puffed onto neurons in layer 2/3 of the somatosensory cortex significantly increased (Fig. 3, G and H).

We next investigated synaptic strength by measuring input/output curves of evoked synaptic responses. We detected no difference in excitatory responses between WT and R451C

KI mice but observed a significant increase in inhibitory responses (~50%) (Fig. 4, A, B, D, and E). Measurements in neuroligin-3 KO mice, by contrast, uncovered no change in inhibitory responses but detected a small, although insignificant, decrease in excitatory responses (Fig. 4, C and F, and fig. S9). This result confirms the finding made in the spontaneous synaptic measurements that the neuroligin-3 R451C KI but not the KO causes a selective increase in inhibitory synaptic transmission. Consistent with the postsynaptic localization of neuroligins (12), we found that the short-term synaptic plasticity properties of inhibitory synapses in neuroligin-3 R451C KI or KO brains did not exhibit a major change (figs. S10 to S12).

Neuroligin-3 R451C KI mice exhibit impaired social behaviors but enhanced spatial learning abilities. To determine whether the changes in synaptic transmission in R451C KI mice produce behavioral impairments, we first tested the mice for global behavioral changes and detected no changes in locomotor activity,

motor coordination, and anxiety-related behaviors in R451C KI mice with a series of tests [dark/light box, open field, novel home cage activity, rotarod, open field arena, and elevated plus maze (fig. S13)].

We next investigated whether R451C KI mice display abnormal social behaviors. R451C KI mice showed no change in the time of interaction with a novel inanimate object. However, the KI mice exhibited a small but significant decrease in interaction with a novel caged adult target mouse compared with interactions of WT littermate controls, indicating a social interaction deficit (Fig. 5, A and B). Similarly, in a test for social versus inanimate preference, R451C KI mice spent significantly less time interacting with a social target than did the WT littermate controls (Fig. 5C). In agreement with a selective effect on social behavior, R451C KI mice spent the same amount of time interacting with an inanimate target as controls during this task. However, when placed into a neutral home cage with a freely moving conspecific juvenile target mouse

Fig. 4. Selective increase in inhibitory synaptic strength in neuroligin-3 R451C KI but not in neuroligin-3 KO mice. Representative traces (A and D) and summary graphs (B, C, E, and F) of synaptic responses induced with increasing stimulus intensities applied with a local microelectrode in acute slices of the somatosensory cortex from littermate pairs of R451C KI mice [(A), (B), (D), and (E)] or KO mice [(C) and (F)]. Recordings were obtained in the whole-cell mode in layer 2/3. EPSCs [(A) to (C)] and IPSCs [(D) to (F)] were analyzed separately after pharmacological isolation. In (A) and (D), arrows and vertical dashed lines indicate peaks measured for determining evoked response amplitude. Dotted horizontal lines represent baselines. All data were recorded in acute slices from littermate R451C mutant and WT mice [data shown are means \pm SEMs; $n = 4$ or 3 littermate pairs for EPSCs (KI or KO) and 5 or 3 littermate pairs for IPSCs (KI or KO); * $P < 0.05$; ** $P < 0.01$ by t test]. For representative traces from the KO mice, see fig. S9; for short-term plasticity measurements in KI and KO mice, see figs. S10 to S13.

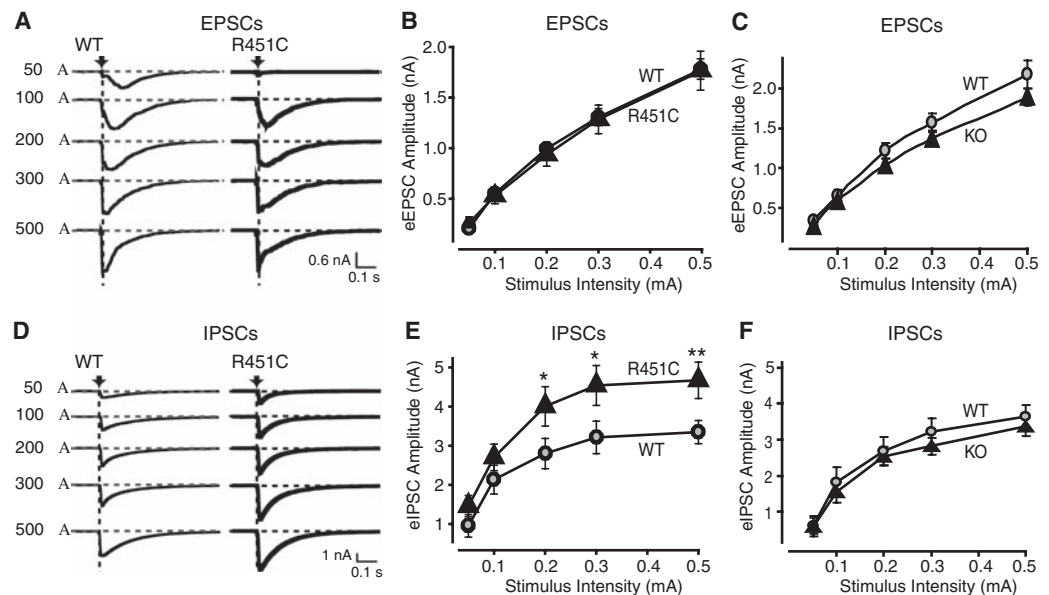
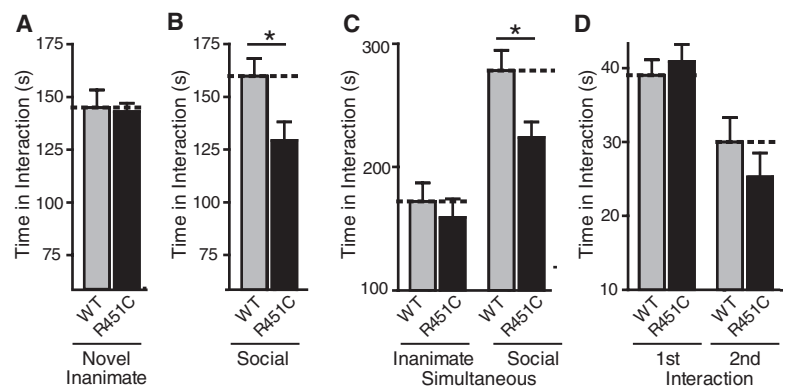


Fig. 5. Impaired social interaction behaviors in neuroligin-3 R451C KI mice. (A) Interacting time of individual WT and R451C KI mice exposed to a novel inanimate object in an unfamiliar cage (5 min). (B) Interacting times of mice that are exposed to an unfamiliar immobilized target mouse in a now-familiar cage [5 min; procedure immediately follows (A)]. (C) Interacting times of mice that are exposed simultaneously to a novel inanimate object and a novel, caged target mouse. (D) Social learning measured by monitoring the times of direct interactions of WT and R451C KI mice with the same freely moving juvenile target mouse on day 1 (first interaction) and day 4 (second interaction for social learning). All data shown are means \pm SEMs; $n = 19$ male littermate pairs; only statistically significant differences between WT and R451C KI mice are specifically identified in the figure (* $P < 0.05$; ** $P < 0.01$; *** $P < 0.001$ by t test or two-way analysis of variance); a detailed statistical analysis for all parameters is provided in table S2 (30).



for 2 min, R451C mutant and WT littermate control mice interacted similarly with the target mouse, presumably because in this test the target mouse initiates the interaction as much as the test mouse, potentially masking social interaction deficits of the test mouse (Fig. 5D). When re-exposed to the same juvenile 3 days later, both the control and the R451C KI mice exhibited a significant decrease in social interaction compared with the initial interaction, demonstrating that the mutant mice recognize the familiar juvenile mouse and are capable of social learning.

Individuals with ASDs exhibit impaired social abilities but can display normal or, rarely, even enhanced cognitive abilities (1–4). To examine whether the selective decrease in social interactions in R451C KI mice is associated with a gain or a loss of other cognitive abilities, we tested spatial learning and memory in R451C KI mice by using the Morris water maze. R451C KI mice learned to locate and mount a visible platform as well as WT littermate control mice did, indicating that basic neurological functions required for swimming, vision, etc. were intact. When the platform was hidden, the R451C KI mice exhibited a significantly enhanced ability to locate the platform (Fig. 6A) and required fewer days of training to learn the location of the platform (Fig. 6B). During the probe trial 24 hours after the seventh day of training, both WT and R451C KI mice displayed a significant preference for the target versus the opposite quadrant, but the R451C KI mice crossed the precise former location of the target platform almost twice as often as their WT littermate controls (Fig. 6B and fig. S14).

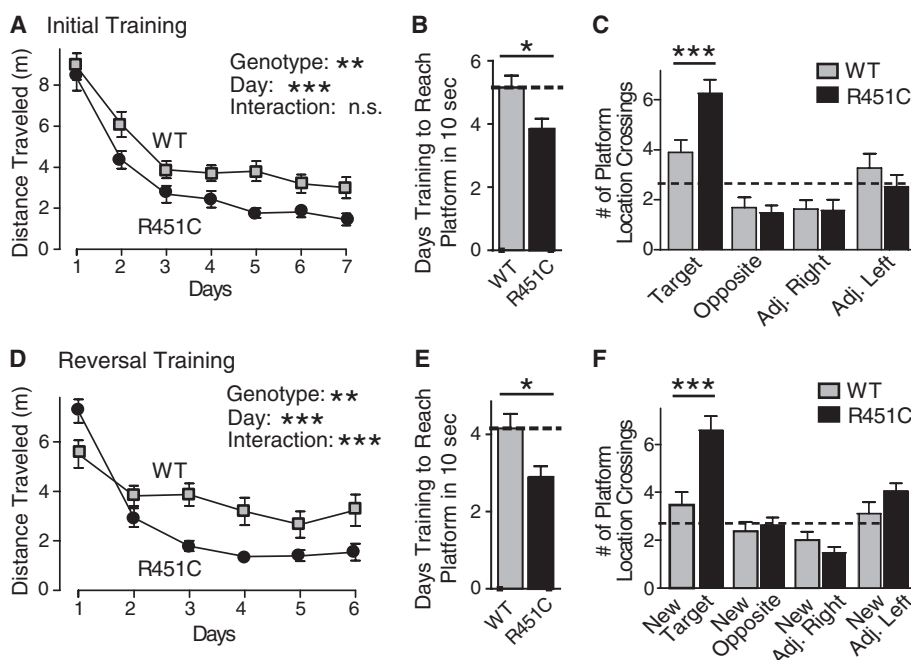
Fig. 6. Neuroligin-3 R451C KI mice exhibit enhanced spatial learning. **(A)** Morris water maze analysis of spatial learning in R451C KI and littermate WT control mice during the initial 7 days of training as measured by the distance traveled to reach a submerged platform [n. s., not significant; * $P < 0.05$; ** $P < 0.01$; *** $P < 0.001$; in (A) and (D), Genotype indicates main effect of genotype; Day, main effect of day of training; and Interaction, interaction between genotype and day.] **(B)** Number of days of initial training required to reach the submerged platform in an average of 10 s or less. **(C)** Number of crossings over the previous location of the target platform and over corresponding locations in the other three quadrants measured on day 8 after removal of the platform (probe trial). **(D)** Reversal learning experiment, in which on day 9 after the probe trial the platform was moved to the opposite quadrant and the learning of the new location of the platform by the mice was monitored. Learning is measured as distance traveled before mounting the newly localized target platform as a function of days of training. **(E)** Number of days of reversal training required to reach the submerged platform in an average of 10 s or less. **(F)** Probe trial after reversal learning uncovers a large increase in spatial learning abilities of the R451C KI mice [dashed lines in (C) and (F) are the mean overall numbers of platform crossings for WT mice]. Only statistically significant differences between WT and R451C KI mice are identified. All data shown are means \pm SEMs; $n = 19$ male littermate pairs; see fig. S14 and table S2 for all statistical comparisons.

To ensure that the increase in number of target location crossings in the R451C KI mice during the probe trial was due to enhanced spatial memory rather than perseveration, we reversed the location of the platform and retrained the same cohort of mice (so-called reversal training). Again, R451C KI mice exhibited a significantly enhanced learning curve during (Fig. 6D) and required fewer days of training to learn the location of the platform (Fig. 6E). Twenty-four hours after the final reversal training day, R451C KI mice displayed enhanced spatial memory during the probe trial. R451C KI mice showed a significant preference for the new target quadrant and spent significantly more time in the target quadrant than did WT littermate control mice (Fig. 6F). Similarly, R451C KI mice crossed the new target location more often than control mice did and exhibited a significant preference for the target location over all other locations, unlike WT mice (Fig. 6F and fig. S14), suggesting that they have an increased ability for spatial learning and memory.

Summary. The phenotype of neuroligin-3 R451C KI mice suggests that this mouse may facilitate for a mechanistic analysis of the pathogenesis of idiopathic ASDs and provide a possible model system to search for more effective treatments for ASDs. We found that the R451C substitution increases inhibitory synaptic transmission without affecting excitatory synaptic transmission and simultaneously impairs social behaviors while selectively enhancing spatial learning abilities. These findings are surprising because ASDs were thought to be associated with a loss of inhibitory drive (29, 31), although a Rett syndrome mouse model also exhibits an

increase in synaptic inhibitory drive (32). The R451C substitution increases inhibitory synapse markers, spontaneous inhibitory event frequency, and the size of inhibitory synaptic responses but does not change short-term synaptic plasticity of inhibitory synapses (Figs. 1 to 3 and figs. S7 and S8), suggesting that the mutation enhances inhibitory synaptic transmission without changing the release probability of these synapses. Thus, our results not only validate the hypothesis that neuroligins act at synapses to specify synaptic properties (20, 33) but also indicate that interfering with the function of a neuroligin alters the excitatory/inhibitory balance in vivo. Moreover, if the mouse model mimics the situation in humans with ASDs, it may be possible to ameliorate autism-related behavioral abnormalities by using attenuation of inhibitory synaptic transmission.

How does the R451C mutation increase inhibitory synaptic transmission? A facile explanation would have been that the destabilization of neuroligin-3 by the R451C substitution (25) and the resulting loss of neuroligin-3 protein produces a loss-of-function of neuroligin-3, which then causes the phenotype. However, our analysis of the neuroligin-3 KO mice rules out this explanation. Although only $\sim 10\%$ of the neuroligin-3 protein remains in the R451C KI mice, this remaining neuroligin-3 protein produces increased inhibitory synaptic transmission, whereas the complete neuroligin-3 KO exerts no such effect. Thus, the R451C substitution likely acts as a gain-of-function mutation, a hypothesis that also explains why no loss-of-function neuroligin-3 mutation was found in humans with ASDs, whereas several loss-



of-function mutations were found in neuroligin-4 in such individuals (22–24).

Our data strongly support the notion that a change in the inhibitory/excitatory balance contributes to the pathogenesis of ASDs. Such a change may alter oscillatory rhythms in brain (34, 35). Given the relatively focused nature of behavioral abnormalities in the R451C KI mice and in some humans with idiopathic ASDs, it is likely that this change is not global but selectively affects only a subset of the many classes of inhibitory interneurons in the forebrain [reviewed in (36, 37)], a question that can now be addressed with the R451C KI mice.

References and Notes

- D. H. Geschwind, P. Levitt, *Curr. Opin. Neurobiol.* **17**, 103 (2007).
- A. M. Persico, T. Bourgeron, *Trends Neurosci.* **29**, 349 (2006).
- American Psychiatric Association, *Diagnostic and Statistical Manual of Mental Disorders: DSM IV* (American Psychiatric Publishing, Arlington, VA, ed. 4, 2002).
- N. O'Connor, B. Hermelin, *Br. J. Psychol.* **80**, 97 (1989).
- P. Moretti, H. Y. Zoghbi, *Curr. Opin. Genet. Dev.* **16**, 276 (2006).
- M. K. Belmonte, T. Bourgeron, *Nat. Neurosci.* **9**, 1221 (2006).
- S. O. Moldin, J. L. Rubenstein, S. E. Hyman, *J. Neurosci.* **26**, 6893 (2006).
- K. Garber, *Science* **317**, 190 (2007).
- K. Ichitchenko, T. Nguyen, T. C. Südhof, *J. Biol. Chem.* **271**, 2676 (1996).
- Y. A. Ushkaryov, A. G. Petrenko, M. Geppert, T. C. Südhof, *Science* **257**, 50 (1992).
- F. Varoqueaux *et al.*, *Neuron* **51**, 741 (2006).
- J.-Y. Song, K. Ichitchenko, T. C. Südhof, N. Brose, *Proc. Natl. Acad. Sci. U.S.A.* **96**, 1100 (1999).
- E. R. Graf, X. Zhang, S. X. Jin, M. W. Linhoff, A. M. Craig, *Cell* **119**, 1013 (2004).
- F. Varoqueaux, S. Jamain, N. Brose, *Eur. J. Cell Biol.* **83**, 449 (2004).
- O. Prange, T. P. Wong, K. Gerrow, Y. T. Wang, A. El-Husseini, *Proc. Natl. Acad. Sci. U.S.A.* **101**, 13915 (2004).
- A. Boucard, A. A. Chubykin, D. Comoletti, P. Taylor, T. C. Südhof, *Neuron* **48**, 229 (2005).
- C. I. Nam, L. Chen, *Proc. Natl. Acad. Sci. U.S.A.* **102**, 6137 (2005).
- K. Futai *et al.*, *Nat. Neurosci.* **10**, 186 (2007).
- B. Cih, S. K. Afridi, L. Clark, P. Scheiffele, *Hum. Mol. Genet.* **13**, 1471 (2004).
- J. N. Levinson *et al.*, *J. Biol. Chem.* **280**, 17312 (2005).
- A. A. Chubykin *et al.*, *Neuron* **54**, 919 (2007).
- S. Jamain *et al.*, *Nat. Genet.* **34**, 27 (2003).
- F. Laumonier *et al.*, *Am. J. Hum. Genet.* **74**, 552 (2004).
- J. Yan *et al.*, *Mol. Psychiatry* **10**, 329 (2005).
- D. Comoletti *et al.*, *J. Neurosci.* **24**, 4889 (2004).
- A. A. Chubykin *et al.*, *J. Biol. Chem.* **280**, 22365 (2005).
- P. Szatmari *et al.*, *Nat. Genet.* **39**, 319 (2007).
- C. M. Durand *et al.*, *Nat. Genet.* **39**, 25 (2007).
- J. L. Rubenstein, M. M. Merzenich, *Genes Brain Behav.* **2**, 255 (2003).
- Materials and methods are available on Science Online.
- J. P. Hussman, *J. Autism Dev. Disord.* **31**, 247 (2001).
- V. S. Dani *et al.*, *Proc. Natl. Acad. Sci. U.S.A.* **102**, 12560 (2005).
- K. Ichitchenko *et al.*, *Cell* **81**, 435 (1995).
- P. J. Uhlhaas, W. Singer, *Neuron* **52**, 155 (2006).
- G. Buzsáki, A. Draguhn, *Science* **304**, 1926 (2004).
- G. Silberberg, S. Grillner, F. E. LeBeau, R. Maex, H. Markram, *Trends Neurosci.* **28**, 541 (2005).
- P. Somogyi, T. Klausberger, *J. Physiol.* **562**, 9 (2005).
- We thank I. Kornblum, J. Mitchell, L. Fan, J. Cormier, and A. Roth for technical support. Supported by grants from the National Institute of Mental Health (R37 MH52804-08 to T.C.S. and K08 MH065975-04 to C.M.P.) and from Autism Speaks (to C.M.P.).

Supporting Online Material

www.sciencemag.org/cgi/content/full/1146221/DC1
Materials and Methods
Figs. S1 to S14
Tables S1 and S2
References

7 June 2007; accepted 23 August 2007
Published online 6 September 2007;
10.1126/science.1146221
Include this information when citing this paper.

REPORTS

Polymer Gate Dielectric Surface Viscoelasticity Modulates Pentacene Transistor Performance

Choongik Kim, Antonio Facchetti,* Tobin J. Marks*

Nanoscopically confined polymer films are known to exhibit substantially depressed glass transition temperatures (T_g 's) as compared to the corresponding bulk materials. We report here that pentacene thin films grown on polymer gate dielectrics at temperatures well below their bulk T_g 's exhibit distinctive and abrupt morphological and microstructural transitions and thin-film transistor (TFT) performance discontinuities at well-defined growth temperatures. The changes reflect the higher chain mobility of the dielectric in its rubbery state and are independent of dielectric film thickness. Optimization of organic TFT performance must recognize this fundamental buried interface viscoelasticity effect, which is detectable in the current-voltage response.

Organic thin-film transistors (OTFTs) have attracted considerable attention as the central components of "printed" electronics (1–3). Moreover, OTFT performance can be substantially enhanced by manipulating the semiconductor/dielectric interfacial properties via optimizing the gate dielectric (4–7). To this end, polymer dielectrics are ideal because of their diverse properties, favorable film-forming char-

acteristics, and tunable surface chemistry for the control of device-critical interfacial trap state densities (8–10). However, whether polymer dielectric chain dynamics affect organic semiconductor growth and OTFT current-voltage (I - V) response has remained unclear.

The glass transition temperature (T_g) of amorphous polymers provides a qualitative measure of chain motion (11–13). At temperatures below T_g , polymers are in a glassy state with little cooperative chain motion, whereas above T_g , polymers enter a rubbery state having substantial chain motion. Relative to bulk materials, T_g is depressed in ultrathin films (14) and in nanoscale pores (15). The extent of T_g depression depends on

the polymer film thickness and substrate/polymer interactions, as characterized by ellipsometry (16), dielectric relaxation spectroscopy (17), Brillouin scattering (18), and fluorescence spectroscopy (19). For extensively studied polystyrene (PS) films on Si or SiO₂ substrates, the empirical Eq. 1 applies (14, 20)

$$T_g(h) = T_g(b) [1 - (A/h)^\delta] \quad (1)$$

where $T_g(h)$ is T_g for a film of thickness h , $T_g(b)$ is the bulk polystyrene T_g (both in degrees kelvin), A is a characteristic length (3.2 nm), and $\delta = 1.8$. The experimental results from which empirical Eq. 1 was derived confer on $T_g(h)$ the meaning of an "average" T_g across the nanoscopic film that is strongly thickness-dependent. For example, a 20-nm-thick PS film with $T_g(b) \sim 100^\circ\text{C}$ exhibits a T_g depression [$\Delta T_g(h,b) = T_g(b) - T_g(h)$] of $\sim 14^\circ\text{C}$, but this effect vanishes ($\Delta T_g(h,b) < 1^\circ\text{C}$) when $h > 100$ nm. Thus, for PS films of thickness > 100 nm, the polymer gate dielectric viscoelastic properties should play little role in OTFT interfacial effects when $T < T_g(b)$. Relations similar to Eq. 1 are applicable to other polymer classes, although parameters A and δ differ and may depend on the substrate [for example, for poly(methylmethacrylate) (PMMA), $A = 0.35$ nm and $\delta = 0.8$ (21); for poly(*t*-butylstyrene) (PTBS), $A = 3.0$ nm and $\delta = 1.05$ (22)]. We show here that when glassy polymeric materials are used as OTFT gate dielectrics, polymer viscoelastic properties strongly influence organic semiconductor film growth, microstructure, and OTFT I - V

Department of Chemistry and the Materials Research Center, Northwestern University, 2145 Sheridan Road, Evanston, IL 60208, USA.

*To whom correspondence should be addressed. E-mail: a-facchetti@northwestern.edu (A.F.); t-marks@northwestern.edu (T.J.M.)